Journal of Civil Aspects and Structural Engineering

www.case.reapress.com

J. Civ. Asp. Struct. Eng. Vol. 2, No. 2 (2025) 113–125.

Paper Type: Original Article

Numerical Investigation of Seismic Behavior of Reinforced Concrete Dams Using the Finite Element Method (Case Study: Manjil Dam)

Iman Zakariyayi[1,*], Tahereh Bonyad Sikaroudi[1]

Department of Civil Engineering, Ayandegan Institute of Higher Education, Tonekabon, Iran; Iman.zakariyayi92@gmail.com; tahere.sigarodi@gmail.com.

Citation:

Received: 03 November 2024 *Revised: 11 January 2024* *Accepted: 23 May 2025*	Zakariyayi, I & Bonyad Sikaroudi, T. (2025). Numerical investigation of seismic behavior of reinforced concrete dams using the finite element method (Case study: Manjil Dam). *Journal of civil aspects and structural engineering, 2*(2), 113-125.

Abstract

Dam construction, as one of the oldest and most complex construction activities, has always been considered by different societies and is also considered one of the important economic resources of each country and region. Concern about the safety of dams has existed for a long time and is increasing day by day. The design and implementation of dams and their safety against earthquakes are of great importance. The main concept of safety is to prevent the failure of a dam and the uncontrolled overflow of the reservoir water with the occurrence of floods, which usually causes greater economic damage to the dam. To assess the safety and stability of existing dams, to determine the adequacy of the proposed reforms for the improvement and upgrading of old dams, and to evaluate the proposed designs for the construction of new dams, it is necessary to evaluate the effects of earthquakes on these dams. Predicting the behavior of concrete dams during earthquakes is one of the most complex and difficult problems in structural dynamics. The overall objective of this study is to numerically investigate the seismic behavior of a concrete dam with a buttress (Case study: Manjil Dam) using the finite element method. ABAQUS software was used for the study. For this purpose, the dam was modeled in two cases A (Dam without a buttress) and B (Dam with buttress). According to the Nonlinear Static Analysis (NSP) of the pushover, comparing the force-displacement diagram of model A and model B, we observed that placing a buttress in model B increased the resistance by 23.45% compared to model A. Also, according to the results obtained, it was observed that the strain contour created by the NSP in the model B sample caused the Tresca shear stress to decrease by an average of 23.97% in the dam body.

Keywords: Buttress dam, Seismic behavior, Finite element method, Manjil Dam.

1 | Introduction

Dam construction, as one of the oldest and most complex construction activities, has always been considered by different societies and is also considered one of the important economic resources of each country and

Corresponding Author: Iman.zakariyayi92@gmail.com

10.48314/jcase.v2i2.56

region from an economic point of view. Dam engineering can be considered a set of important technical and basic sciences that together make the design and implementation of the dam possible and examine the dam structure in terms of incoming loads and resistance to destructive factors. The design and implementation of dams is such that if factors such as sedimentation of the reservoir, etc. do not exist, there will be no limit to the life and time period of operation of the dam. For several decades, it has been recommended to build dams safely and economically, as well as quickly, in order to increase energy production. The critical problem that we are expected to face in recent years is the increase in the life and wear of dams [1].

In Iran, due to the problems caused by water shortage and specific climatic conditions, water has always been considered a very valuable and strategic material, so this issue has caused the construction of dams, dams and other water storage and transfer facilities to have a special appearance in the works left behind in Iranian culture and civilization. The Achaemenid kings, due to the geographical needs of the country of Iran and the interest they showed in the expansion and development of the land under their rule, built many dams and dams in the southwestern and southern parts of Iran during their empire. Many of the water supply and irrigation systems that were used in Iran for many years are due to the efforts of Iranian engineers and craftsmen who tried in very distant times to meet the needs and deficiencies in the fields of development and development, and their works and evidence can also be understood in different parts of Iran. In addition, many of the works left behind from this era can also be seen in the lands subordinate to the ancient Iranian governments.

Concerns about dam safety have long existed and are increasing day by day. The design and construction of dams and their safety against earthquakes are of great importance [2]. Since 1928, with the failure of a large number of different dams, the risk of failure of large dams seemed obvious. Most of the failures that occurred in dams occurred due to failures in our foundations. To answer the question of why we need to retrofit, we must answer that: 1) earthquakes are a real and threatening phenomenon, 2) retrofitting saves many lives, and 3) it reduces the economic impact of total failure and the cost of repairs and the risks of service interruption. The fact that large dams have failed during earthquakes and that many lives have been lost may be an incentive for dams to be designed and constructed to be safe against earthquakes. Large dams are among the first structures for which seismic design criteria were considered since 1930. Since 1989, the International Board on Large Dams has been waiting for the code of selection of seismic design parameters for concrete dams. According to this code, the design against earthquakes was quasi-static and with a horizontal acceleration of 0.1 g. A new phase of seismic analysis of dams began in 1971 with the San Fernando earthquake in California, which caused serious damage to earth dams and also to gravity arch dams. Therefore, in a dam with a serious vulnerability, the level of seismic safety must be sufficient to withstand more severe ground movements at the site of the structure. Strong earthquakes have occurred in Iran in 2003, Sumatra in 2004, Kashmir in 2005 and several in Japan. Although these earthquakes may cause problems for vulnerable dams, these events have shown that earthquake hazards exist as long as the safety of dams is unknown and there is still a serious threat to them.

The more severe ground motions that result from surface earthquakes at dam sites can have accelerations greater than the old design acceleration of 0.1 g. The maximum ground motion acceleration of 1 g at the foundation in areas of high seismicity is produced by earthquakes with a surface center and magnitude of 2.7. It is therefore necessary to explain that there is a discrepancy between the maximum measured earthquake acceleration and the accelerations used for the design of a dam. A very large number of seismic behaviors are now known. It is necessary to collect and use complete information from all dams. It is still much better to design and implement a dam well than to have it need to be repaired and reinforced after an earthquake or to fail altogether. A dam design that is considered safe today may not be safe forever in the future and in the event of stronger earthquakes.

In 2017, Khiavi et al. [1] studied concrete gravity dams with damper systems using probabilistic methods. The results of this study showed that the rubber damper reduced the principal tensile stress on the dam body relative to the concrete reinforcement at most points of the dam heel.

Komasi and beiranvand [3] analyzed the Ayushman Dam using a numerical method in 2019. The results of this study showed that the water pressure height on the downstream side of the dam curtain had a sudden drop in the results of precision instrumentation and numerical modeling, indicating the proper functioning of the dam curtain.

Sadeghi and Moradloo [4] in 2022 studied concrete dams damaged by earthquakes. Using the finite element method based on the standard code approach and numerical software, they evaluated the seismic response of concrete gravity dams. Their findings indicate that the dam crest displacements for the dam foundation system are 562.5 mm greater than for the dam system.

Aureli et al. [5] in 2021 used a numerical method to study the effect of a historic dam failure in Italy. In this study, various geometric and material nonlinear behavior models were compared for the analysis of arched concrete dams. In the recent study, the difference in the application of different plastic behavior models for concrete in the range of small and large displacements was first stated, and then a parametric analysis was performed on the results of the sensitivity calculations. To achieve the above goals, the Malpasse arched concrete dam model, which was destroyed in the 1950s, was used. In the aforementioned analyses, the interaction between the dam and the foundation was taken into account and the loading was continued statically until the destruction limit of parts of the foundation and the body. The same plasticity criteria were used to model the nonlinear behavior of the dam and the foundation. Among these models, the Saint-Venant-Kirchhoff and Neo-Hawkin models were selected for the geometric nonlinear state and were used in the analyses.

Bharti et al. [6] analyzed a gravity concrete dam using a numerical method in 2023. In this study, a study was conducted using dynamic analysis of a gravity concrete dam due to an earthquake. Abaqus software was used in this modeling. This software has a high ability to analyze structures and the interaction between the structure and the reservoir, and also provides a better understanding of the behavior of the structure in different earthquakes by modeling the real behavior of materials and the real form of loading. Considering boundary conditions allows for more accurate determination of stresses and displacements in different parts of the dam. On the other hand, dynamic analysis has been used in this study to understand the safety of the structure under different earthquakes more clearly. The results indicate that earthquakes with vertical acceleration can disrupt the stability of these dams, and we see larger stresses in the upstream part than in the downstream part.

Saksala and Makinen [7] used a numerical method to investigate cracks in gravity dams under static and dynamic loads. In this paper, a computer program has been organized to simplify the problem and the dam-foundation interaction has been investigated. In this program, the dam body and foundation rock, which are modeled in 3D, are divided by finite elements. It is worth noting that the results of the method used in this study are very close to the relatively complex models of previous studies. In addition, the aforementioned program is able to use the damping solvent extraction method. Also, in this study, the effect of the damping solvent extraction method on increasing the convergence of the dynamic response of gravity concrete dams was also investigated. Given the vital role of dams in water resource management, power generation, flood control, and drinking and agricultural water supply, the safety of these structures is of great importance, especially against natural phenomena such as earthquakes. Among natural hazards, earthquakes are considered one of the most important factors threatening the safety of concrete dams due to their unpredictable nature and high destructive intensity. Past experiences have shown that although rare cases of dam failure due to earthquakes have been reported, the possible destruction of these structures can lead to irreparable economic, social, and environmental losses. Therefore, a full reservoir at the time of an earthquake is considered a critical state in safety analyses. The behavior of concrete dams against earthquakes is affected by various factors, including material strength, stress distribution, boundary conditions, and dynamic interaction with reservoir water and foundation. Accurate prediction of the behavior of these structures during earthquakes is one of the most complex issues in the field of structural dynamics, as it includes phenomena such as joint slippage, concrete cracking, water separation from the dam body, vacuity, and the complex interaction of the dam and

reservoir. These phenomena are nonlinear in nature, and their correct simulation requires advanced numerical analyses and consideration of hydrodynamic effects dependent on frequency and water compressibility. Given these complexities and the high importance of dam safety, it is essential and inevitable to study the seismic behavior and analyze the dynamic response of concrete dams, both in the design phase of new dams and in the rehabilitation and upgrading of existing dams. The results of these analyses can lead to the development of effective solutions in risk management, planning for emergency situations, and selecting appropriate rehabilitation methods. Therefore, a detailed study and assessment of the behavior of concrete dams under seismic loads is a fundamental necessity in order to ensure operational safety, reduce damage from natural disasters, and maintain the functional stability of these key national infrastructures.

2 | Research Method

2.1 | Statistical Population, Sampling Method and Sample Size

I. Obtaining records and accelerometers of major earthquakes in the world in order to be based on the numerical simulation of the Manjil Dam.

II. Necessary sampling for the geometric characteristics of the dam, concrete type and reinforcement.

2.2 | Numerical Simulation of the Seismic Behavior of the System

The formulation of the numerical analysis of the problem is dynamic in the time interval, which will be converted to static analysis if a very long time step is applied. The numerical program is written in Fortran 90 and has an analysis capability including "coupling of fluid and solid environments", "nonlinear behavior of materials and failure model of rock and concrete materials", "nonlinear contact behavior of the common boundary of separate environments, large contraction joints, joints and faults"[8]. The general nonlinear equation of body motion is

$$\left[k_t + \frac{\gamma}{\beta\Delta t}[G_T] + \frac{1}{\beta\Delta t^2}[M]\{\ddot{U}_{n+1}\}\right. = \{R_{n+1}\} + [C]\left\{\frac{\gamma}{\beta\Delta t}\{U_n\} + \left(\frac{\gamma}{\beta} - 1\right)\{\dot{U}_n\} + \Delta t\left(\frac{\gamma}{2\beta} - 1\right)\{\dot{U}_n\}\right\} + [M]\left\{\frac{1}{\beta\Delta t^2}\{U_n\} + \frac{1}{\beta\Delta t}\{\dot{U}_n\} + \left(\frac{1}{2\beta} - 1\right)\{\dot{U}_n\}\right\}, \quad (1)$$

where [M], [C], and [K] are the mass, damping, and stiffness matrices, respectively, and {R} is the vector of unbalanced forces due to nonlinear effects. {U}, {Ů}, and {Ü} are the velocity and acceleration displacement vectors, respectively, and {KT} is the tangential stiffness matrix, and [CT] is the updated damping matrix due to the reduction in stiffness at each time step. The damping matrix is determined by the well-known Rayleigh relation. The Newmark method is used for numerical integration of the equation of motion [9], [10]. The full Newton method is also used in the iterative problem [11]. The parameters β and У are chosen as the determinants of stability and analytical accuracy as $\beta = 1/4$ and $У = 1/2$. In this modeling, the Lagrangian method is used to model the fluid part. Also, the volume of sediments at the bottom of the reservoir is related to the physical and mechanical characteristics and is considered in the Lagrangian method. To determine the stiffness matrix of fluid elements including water and reservoir sediments, the volumetric pressure-strain relationship is used in the form of *Eq. (2)*.

$$P = \lambda\varepsilon_u \quad (2)$$

where P, λ, and ε_u are the average stress, bulk modulus, and volumetric strain of the fluid, respectively. The volumetric strain as a function of the displacement of the nodal points is given by *Eq. (3)*.

$$\varepsilon_{\upsilon} = \frac{\partial u_x}{\partial x} + \frac{\partial u_y}{\partial y} + \frac{\partial u_z}{\partial z} \quad (3)$$

where μ_{χ}, μ_{γ}, and μz are the displacement components in three directions, respectively. The main problem of modeling mobile behavior using the Lagrangian method compared to the Eulerian method is the creation of spurious models due to the selection of zero shear modulus [12].

2.3 | Details of Modeling Group A, B Shaped Samples in the Finite Element Software Environment

As we know, in this study, we use two model samples called models, A, B, so the finite element software ABAQUS was used to model the designed samples. The SOLID element was used to model concrete, and the shell element was used to model steel sections. In the stage of introducing material characteristics in the ABAQUS software, the behavior of materials in the linear and nonlinear regions was considered. Also, the mechanical characteristics of mild steel ST 37) and concrete with a compressive strength of 47.6 MPa were used. Also, the Tie constraint was used to connect all the welded edges to each other, and the Contact constraint was used to define the surface condition of all the surfaces in contact with each other on a surface-to-surface basis [13].

Table 1. Accelerogram specifications used in this study.

Row	Introducing the Accelerator	Time Step Δt	Great M	Distance from Station (km)
1	The Manjil accelerator	0.005	7.3	19.65
2	The Kobe accelerator	0.005	7.6	39.12
3	The Elsentro accelerator	0.005	6.9	98.14
4	The Tabas accelerator	0.005	7.3	46.18
5	The North Bridge accelerator	0.005	6.5	68.20
6	The Loma accelerator	0.005	6.7	18.13
7	The Chichi accelerator	0.005	7.2	98.10

2.4 | Modeling of Model A, B, in ABAQUS/CAE

As mentioned, ABAQUS/CAE is the main and graphical environment of ABAQUS, in which various capabilities are available for modeling, executing the solution command and monitoring it simultaneously, and also viewing the results. ABAQUS/CAE is divided into ten environments, in each of which one of the modeling sections is performed according to a logical process. When the modeling is completed, ABAQUS/CAE creates an input file that, as mentioned earlier, has a structure very similar to a programmed code and is analyzed by one of two implicit or explicit methods. The software solver reads the input file and sends information to the CAE during the solution process, which enables the ability to monitor the solution process simultaneously. The analysis results are also stored in an output file. Finally, the user opens the solver output file using the Visualization environment and views the results as a graph, contour, animation, or any other graphical interface.

2.5 | Creating Model Geometry in the PART Environment

Parts are the building blocks of a model in CAE ABAQUS. The Part environment is used for geometric modeling of these blocks. In this environment, geometric modeling of parts is performed. For modeling concrete parts, we used the 3D SOLID command of the EXTUDE type. After that, the following concrete shapes were drawn and defined through the geometric specifications of the model in the SCKETCH environment. We used the SHELL command to define the steel of these sections. After defining the rebars in the following shapes, we can see the graphic view of the steel sections after they are created in the ABAQUS

program's graphic environment. We can see the parts created for the study model geometry used in this modeling in the following shapes.

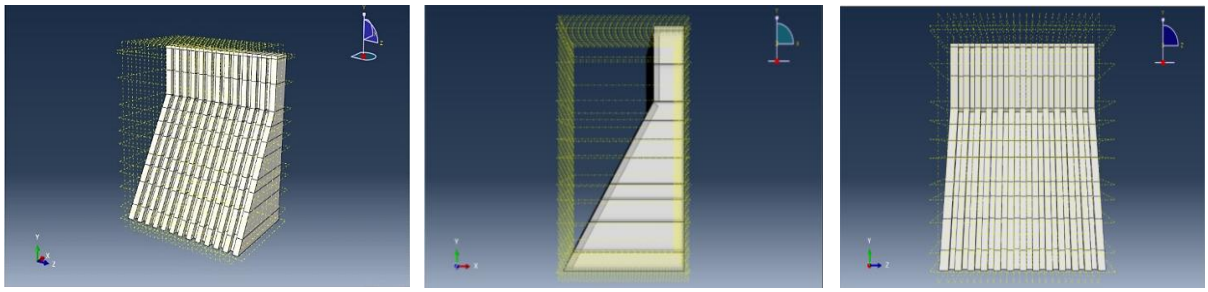

Fig. 1. View of the parts created in the study model in the graphical environment of the Abaqus program.

2.6|Mechanical and Thermal Parameters and Definition of Materials in the Property Environment

Material specifications are defined for this study for models A, B, The modulus of elasticity of steel in this modeling for sample A is 199 Gpa, and the concrete used in this modeling is concrete with confined behavior with a compressive strength of 47 MPa for samples A, B.

For this purpose, in this workspace, the properties of the analyzed materials are defined, the profile of the beam cross-section is defined, the properties defined are assigned to the parts, etc. After defining the materials based on the specifications defined in the previous chapter, in this module, I define the materials. After defining the materials and correctly assigning the desired model in the ABAQUS graphical environment, it turns green. In the following figures, we can see the assignment of materials to the desired model. We can see the parts created in the PART environment in the PROPERTY module, assigning materials to each part of the study model in this module, which is colored green after assigning materials [14]. We can see all these details in *Fig. 2* below. The values of the mechanical and thermal parameters applied in this analysis are as follows.

Table 2. Mechanical and thermal properties of concrete.

	Concrete	Cornerstone
Density	2400 kg/m^3	2000 kg/m^3
Modulus of elasticity	40 GPa	25 GPa
Poisson's ratio	0.2	0.25
Thermal conductivity	226368 J/m^2/C/day	-
Thermal expansion coefficient	6 ×10 $^{-6}$ /°C	8×10^{-6} /°C
Specific heat	912 J/m^3/C	2000 J/m^3/C

3|Findings

3.1|Visualization Environment

After the analysis is performed using one of the two Standard Explicit methods, the Visualization environment should be used to view the solution results. If you run ABAQUS/Viewer, the same CAE window will appear, except that it only has the Visualization environment. In the figures below, we can see the output and various meters of the analysis parameters of the study model.

After analyzing the A models in the Visualization environment, we can see the meters of the various analysis parameters. In the figure below, we can see the displacement meter of the A model sample.

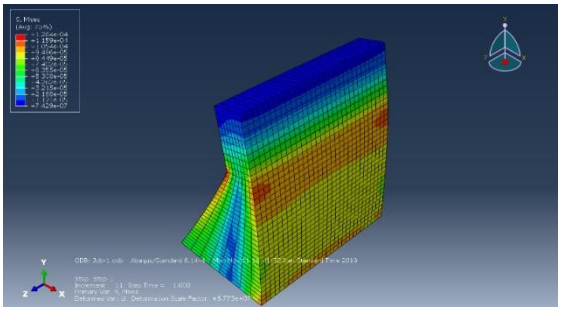

Fig. 2. Magnitude displacement distribution in the study model.

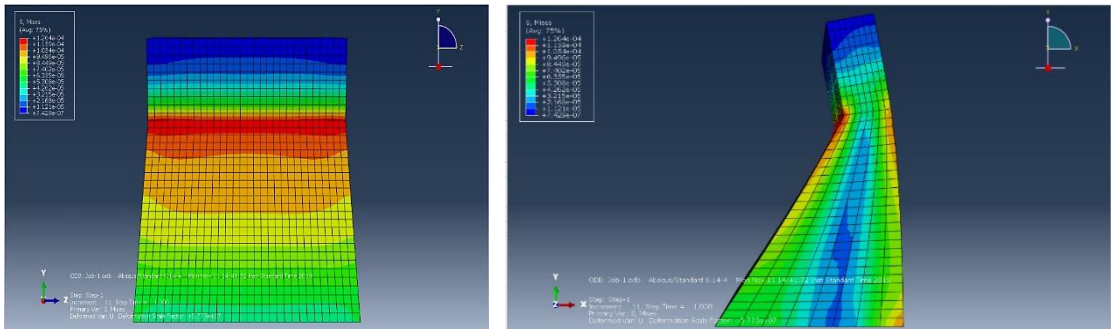

Fig. 3. Distribution of U-magnitude displacement in the study model.

3.2 | Output Results from Nonlinear Static and Dynamic Analysis Linear Time History Dynamic Response Resulting from Nonlinear Static Analysis and Linear Time History Analysis of Sample A

In this section, we subject the studied dam model A, which is without a heel, to seven earthquake records, and we continue this analysis until the state that has the greatest positive effect in reducing the dynamic response. After that, we subject the structure under consideration to nonlinear static pushover analysis. After analyzing the force-displacement diagram (Pushover curve) and the history diagram of the structure displacement, base shear, and acceleration of model A under seven earthquake records, we can see the history diagram of the displacement of model A under seven earthquake records, which is a near-fault earthquake, in *Fig. 4*, resulting from the linear analysis (Time history).

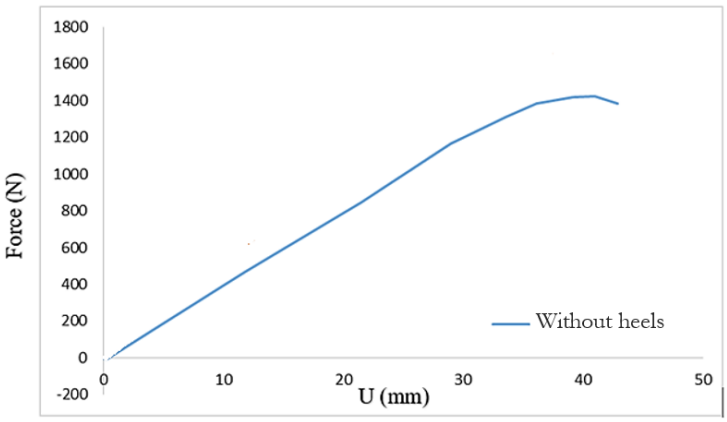

Fig. 4. Force-displacement diagram of model A.

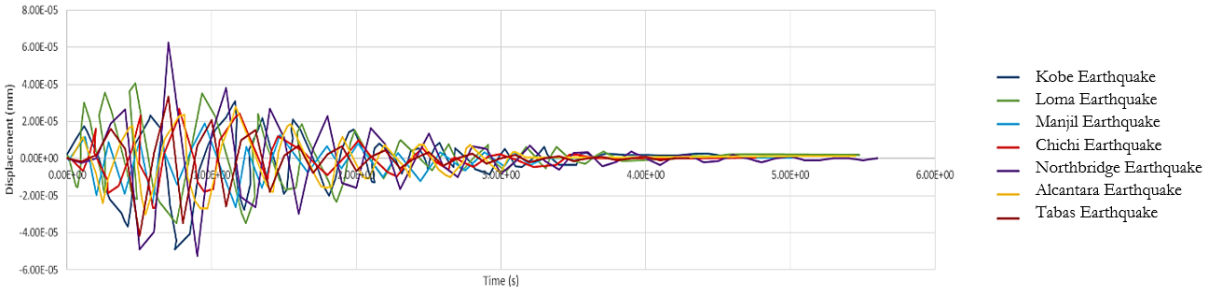

Fig. 5. Time history diagram of displacement of model A under seven earthquake records.

We see the history diagram of the base shear of model A under seven earthquake records, which is a near-fault earthquake, in *Fig. 5* resulting from linear analysis (Time history).

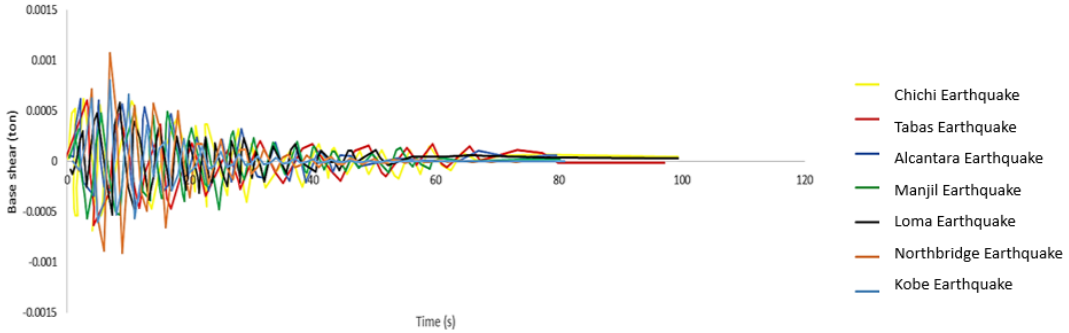

Fig. 6. History of base shear of model A structure under seven earthquake records.

We see the acceleration diagram of model A structure under seven earthquake records, which is a near-fault earthquake, in *Fig. 6* resulting from linear analysis (Time history).

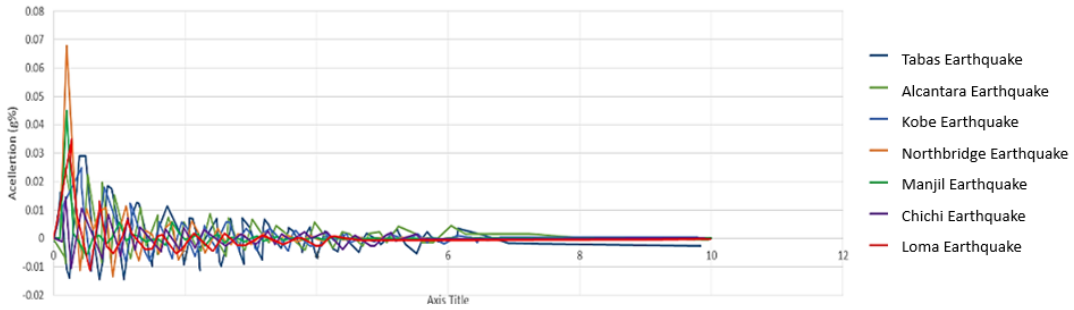

Fig. 7. Acceleration history diagram of model A structure under seven earthquake records.

3.3|Dynamic Response Resulting from Nonlinear Static Analysis and Linear Time History Analysis of Model B

In this section, we subject the studied dam model B, which is with a heel, to seven earthquake records, and we subject this analysis to a state that has the greatest positive effect in reducing the dynamic response. After that, we subject the structure under consideration to a nonlinear static pushover analysis. After analyzing the force-displacement diagram (Pushover curve) and the structural displacement history diagram, we can observe the results of the linear analysis (Time history) of model A under seven earthquake records.

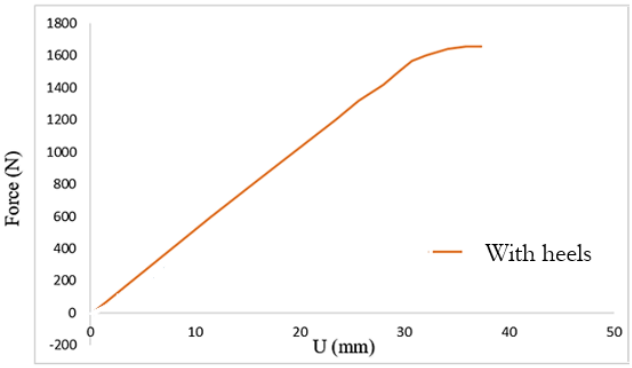

Fig. 8. Force-displacement diagram of model B.

In this section, model B, the dam under study with a heel, is subjected to seven earthquake records, subjected to linear time history analysis, and this analysis is continued until the state that has the greatest positive effect in reducing the dynamic response. After that, we subject the structure under consideration to a nonlinear static pushover analysis. After analyzing the force-displacement diagram (Pushover curve) and the history diagram of the structural displacement, base shear, and acceleration of the model of study group B under seven earthquake records resulting from linear analysis (Time history) is shown in *Fig. 6*.

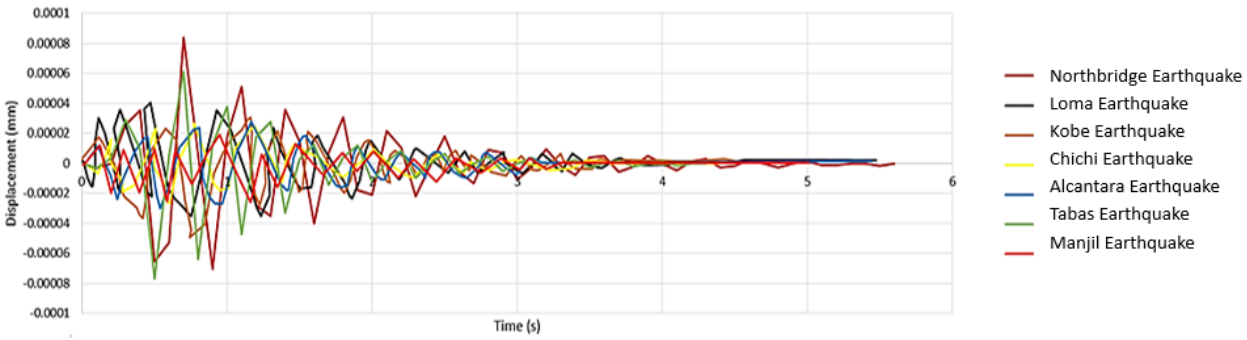

Fig. 9. Time history diagram of displacement of model B under seven earthquake records.

We see the history diagram of the base shear of model B under seven earthquake records, which are earthquakes in the near-fault area, in *Fig. 7* resulting from linear analysis (Time history).

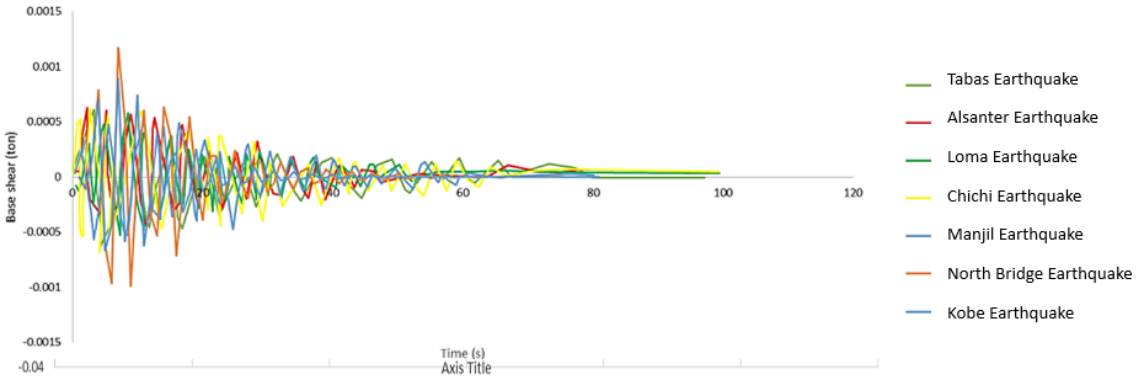

Fig. 10. Historical shear diagram of model B base under earthquake (Seven record earthquakes).

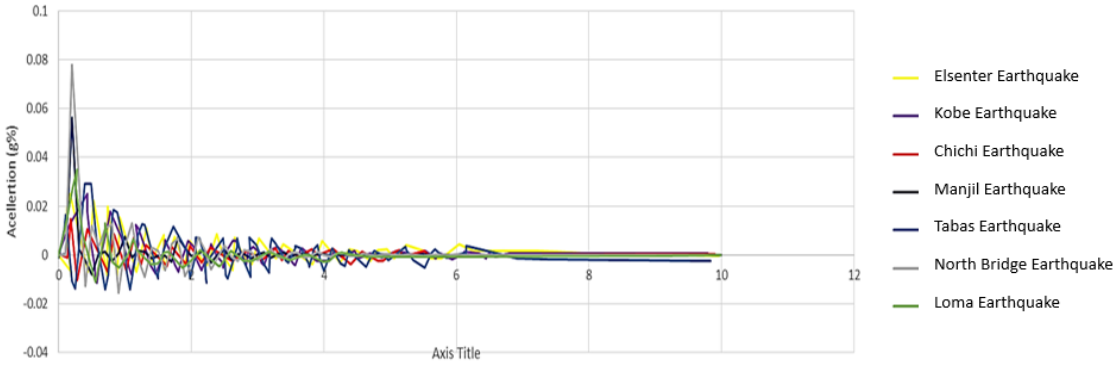

Fig. 11. Acceleration history diagram of model B structure under seven earthquake records.

3.4 | Comparison of the Results of Nonlinear Static Analysis and Dynamic Time History Analysis of Models A and B

In this section, we compare the results of models A and B, which are with and without heel, respectively, under seven earthquake records, which are near-fault earthquakes resulting from linear analysis (Time history), and then subject the two models A and B to nonlinear static pushover analysis.

After performing linear analysis and nonlinear analysis of these two models, we can compare the force-displacement diagrams (Pushover curve) and the history diagram of structural displacement, base shear, and acceleration of models A and B.

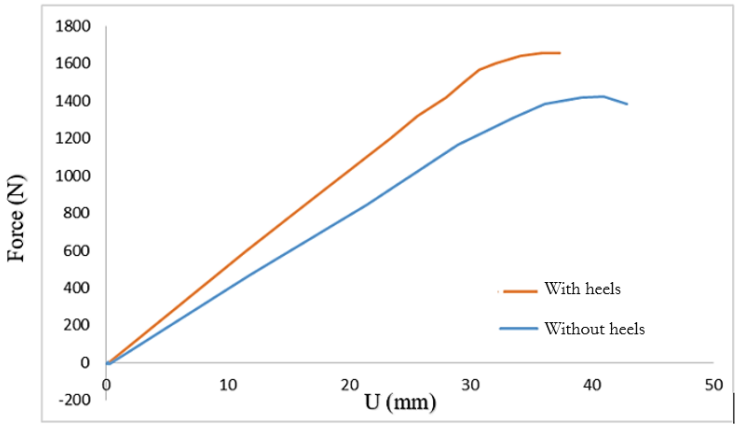

Fig. 12. Force-displacement curve of model A and model B.

3.5 | Comparison of the Results of Dynamic Analysis of Time History of Models A and B

In this section, we compare the results of models A and B, which are respectively with heel and without heel, under seven earthquake records, which are earthquakes near the fault due to linear analysis (Time history), and subject them to linear time history analysis. After performing linear analysis (Time history), we can see the comparison of the graphs of the history of structural displacement, base shear, and acceleration of models A and B.

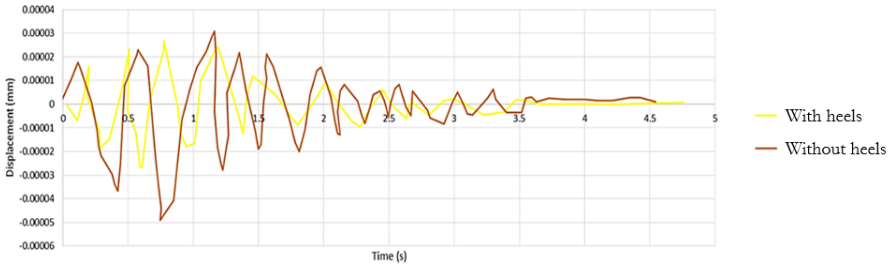

Fig. 13. Comparison of the time history chart of the displacement of models A and B.

We can see the comparison of the base shear history diagram of model A and B under seven earthquake records, which is a near-fault zone earthquake, in *Fig. 12* resulting from linear analysis (Time history).

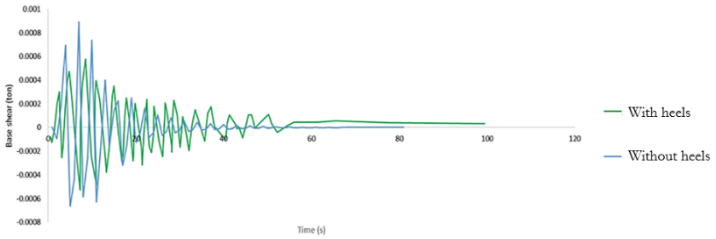

Fig. 14. Comparison of the time history chart of the base cut of models A and B.

We can see the comparison of the acceleration history graph of model A and B structures under seven earthquake records, which is a near-fault zone earthquake, in *Fig. 14* resulting from linear analysis (time history).

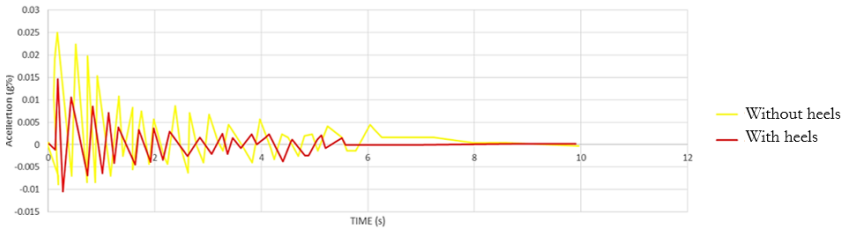

Fig. 15. Comparison of the acceleration time history diagram of the structure of Models A and B.

After analyzing models A and B in the Visualization environment, we can view graphs of various analytical parameters. In the figure below, we can see the hysteresis graph under barcyclic loading for models A and B.

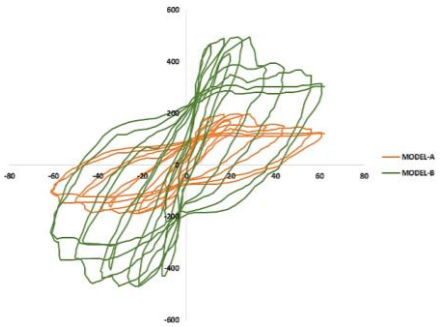

Fig. 16. Hysteresis diagram of model A, B under cyclic loading.

4 | Conclusion

As seen in this study, we use two model samples called models B and A, so the ABAQUS finite element software was used to model the designed samples. The SOLID element was used to model the concrete, the shell element was used to model the steel sections, and the WIRE element was also used to model the rebars. In the stage of introducing the material specifications in the ABAQUS software, the behavior of the materials in the linear and nonlinear regions was considered. After modeling and performing finite element analyses, the following results were obtained in this study.

I. According to the nonlinear static analysis of pushover, comparing the force-displacement diagram of model A (Dam without heel) and model B (Dam with no heel), we observed that placing a heel in model B increased the resistance by 23.45 percent compared to model A (Dam without heel).

II. According to the comparison of the displacement time history chart of model A (Dam without heel) and model B (Dam with heel), we observed that by placing the heel in model B, the resistance decreased by 23.45%.

III. According to the comparison of the base shear history chart of model A (Dam without heel) and model B (Dam with heel), it was observed that by placing the heel in the model B sample, the resistance decreased by 18.36%.

IV. According to the comparison of the base acceleration history chart of model A (Dam without heel) and model B (Dam with heel), it was observed that by placing the heel in the model B sample, the resistance decreased by 23.45%.

V. According to the comparison of the pushover history chart (Nonlinear Static Analysis (NSP)) of model A (Dam without heel) and model B (dam with heel), it was observed that by placing the heel in the model B sample, the ductility decreased by 20.31%.

VI. According to the comparison of the pushover history graph (NSP) of model A (Dam without heel) and model B (Dam with heel), it was observed that by placing the heel in the model B sample, it caused a 14.52% stiffness.

VII. According to the comparison of the pushover history graph (NSP) of model A (Dam without heel) and model B (Dam with heel), it was observed that by placing the heel in the model B sample, it caused an 18.75% hysteresis energy absorption.

VIII. According to the comparison of the von Mises stress contour (NSP) of model A (Dam without heel) and model B (Dam with heel), it was observed that by placing the heel in the model B sample, the von Mises stresses in the dam body decreased by an average of 19.87%.

IX. According to the comparison of the resulting von Mises stress contour (NSP) of model A (Dam without heel) and model B (Dam with heel), it was observed that by placing the heel in the model B sample, the resulting von Mises stresses decreased by an average of 19.87 percent in the dam body.

X. According to the comparison of the resulting strain contour (NSP) of model A (Dam without heel) and model B (Dam with heel), it was observed that by placing the heel in the model B sample, the resulting strain stresses decreased by an average of 17.63 percent in the dam body.

XI. According to the comparison of the resulting strain contour (NSP) of model A (Dam without heel) and model B (Dam with heel), it was observed that by placing the heel in the model B sample, the resulting Tresca shear stress decreased by an average of 23.97 percent in the dam body.

Funding

This research received no external funding.

Data Availability

The data used in this study are available from the corresponding author upon reasonable request.

Conflicts of Interest

The authors declare no conflict of interest.

Authors' Contributions

I. Z.: Research Design, Data Curation, Writing-original draft, Methodology, Visualization, Software. T. B. S.: Conceptualization, and Formal Analysis, Validation, and Investigation, Writing-Review & Editing, and Validation. The authors have read and agreed to the published version of the manuscript.

Consent for Publication

Consent for publication has been obtained from the authors.

Ethics Approval and Consent to Participate

The authors confirm that this research did not involve human participants or animal subjects.

References

[1] Khiavi, M. P. (2017). Investigation of seismic performance of concrete gravity dams using probabilistic analysis. *Gradjevinar*, *69*(1), 21–29. https://doi.org/10.14256/JCE.1454.2015

[2] Mohammadnezhad, H., Ghaemian, M., & Noorzad, A. (2019). Seismic analysis of dam-foundation-reservoir system including the effects of foundation mass and radiation damping. *Earthquake engineering and engineering vibration*, *18*(1), 203–218. https://doi.org/10.1007/s11803-019-0499-4

[3] Komasi, M., & beiranvand, B. (2020). Study of seepage flow and cutoff wall performance of eyvashan earth dam using numerical analysis. *Water resources engineering*, *13*(47), 1-14. (**In Persian**). https://wej.marvdasht.iau.ir/article_4456.html?lang=en

[4] Sadeghi, M. H., & Moradloo, J. (2022). Seismic analysis of damaged concrete gravity dams subjected to mainshock-aftershock sequences. *European journal of environmental and civil engineering*, *26*(6), 2417–2438. https://doi.org/10.1080/19648189.2020.1763475

[5] Aureli, F., Maranzoni, A., & Petaccia, G. (2021). Review of historical dam-break events and laboratory tests on real Topography for the validation of numerical models. *Water*, *13*(14), 1968. https://doi.org/10.3390/w13141968

[6] Bharti, M. K., Sharma, M., & Islam, N. (2020). Study on the dam & reservoir, and analysis of dam failures: A data base approach. *International research journal of engineering and technology (IRJET)*, *7*(5), 1661–1669. https://www.academia.edu/44198068

[7] Saksala, T., & Mäkinen, J. (2020). Numerical modelling of cracking in gravity dam under static and seismic loadings with multiple pre-embedded discontinuity FEM. *Procedia structural integrity*, *28*, 784–789. https://doi.org/10.1016/j.prostr.2020.10.091

[8] Fenves, G., & Chopra, A. K. (1985). Effects of reservoir bottom absorption and dam-water-foundation rock interaction on frequency response functions for concrete gravity dams. *Earthquake engineering & structural dynamics*, *13*(1), 13–31. https://doi.org/10.1002/eqe.4290130104

[9] Chopra, A. K. (2022). *Dynamics of structures*. Pearson. https://www.amazon.com/Dynamics-Structures-3rd-Anil-Chopra/dp/8131713296

[10] Zienkiewicz, O. C., & Taylor, R. L. (2005). *The finite element method for solid and structural mechanics*. Elsevier.

[11] Bathe, K. J. (1996). Finite element procedures. https://B2n.ir/xp8255

[12] Hughes, T. J. R. (2000). *The finite element method: Linear static and dynamic finite element analysis*. Courier Corporation. https://www.amazon.com/Finite-Element-Method-Mechanical-Engineering/dp/0486411818

[13] Liu, Y., Chen, D., Pan, Z., Hu, H., & Liu, Y. (2024). Nonlinear seismic analysis of concrete dams using ABAQUS-based scaled boundary finite element method. *Journal of earthquake engineering*, *28*(15), 4209–4240. https://doi.org/10.1080/13632469.2024.2383778

[14] Bas, B. E. (2020). *Study on the thermal properties of concrete containing ground granulated blast furnace slag, fly ash and steel reinforcement*. West Virginia University. https://www.proquest.com/openview/80df5f1d82b93dd8c96d180720021dd3